Materials for Integrated of THz sensors in EWOD chips

Lilian Sirbu[1], Raluca Muller[2], Mihai Danila[2], Vasilica Schiopu[2], Alina Matei[2], Florin Comanescu[2], Angela Stefan[3], Angela Baracu[2], Traian Dascalu[3]

1. *Institute of Electronic Engineering and Nanotechnologies "D. Ghitu"*, 3/3, *Academiei str., MD-2028 Chisinau, Moldova,* sirbu_lilian@yahoo.de
2. *National Institute for R&D in Microtechnologies- IMT Bucharest, Erou Iancu Nicolae 126 A str., Bucharest, Romania,* Raluca.Muller@IMT.ro
3. *National Institute for Laser, Plasma and Radiation Physics Laboratory of Solid-State Quantum Electronics, PO Box MG-36, Magurele, 077125, Romania*

***Abstract* — We developed a technology for deposition of metal contacts/wires upon nanoporous InP thin film structures and RF sputtered InP films. Indium phosphide (InP) films were deposited onto glass substrate using RF magnetron sputtering by varying the substrate temperature (50–100°C), under constant argon pressure (6.3•10^{-3} Bar) and RF power (40-100 W).**

***Index Terms* — *InP film, LT-InP, terahertz (THz) spectroscopy, THz-TDS, ZnO*.**

4. INTRODUCTION

The THz radiation can be produced by various methods (free electron lasers, quantum cascade lasers, Gunn diode, etc) and in different forms (continuous wave, pulsed, monochromatic, broadband). The scope of this work is a broadband short pulse THz radiation generated in photoconductive antenna, see figure 1.

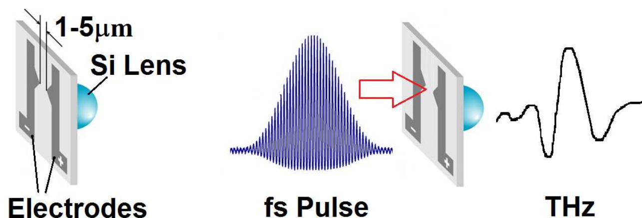

Fig. 1. THz antenna.

A short optical pulse (fs) generates charges in a semiconductor area between two surface electrodes . These charges are accelerated in the electrical field applied between electrodes and recombining very rapidly (because of structural defects) generate broad band THz pulses into the 0.1-5 THz range.

The application areas for THz technologies are rapidly expanding, and this stimulates the need for efficient THz sources. THz emission from semiconductor surfaces was investigated previously in connection with transient photocurrents that radiate THz fields as well as in the context of nonlinear optics. Up to now a low temperature grown GaAs (LT-GaAs) was successfully used for this kind of photoconductive antennae, while other materials and methods are shown to be less efficient or have not been enough studied). One of the promising materials though, as well as LT-GaAs, is a LT-InP and nanostructured InP.

In analogy with many similar applications of both optical and microwave radiation, terahertz radiation can be used for imaging and sensing. The unique properties of terahertz radiation include the transparency of common packaging materials such as glass and plastics for drugs detection, as well as tissues and skin, for medical applications. The sub-millimetre wavelength permits imaging with a diffraction-limited resolution similar to that of the human eye, and many of the proposed target substances exhibit unique spectral fingerprints in the terahertz range, which can be used for identification and chemical analysis [1].

5. DEVICE FABRICATION & RESULTS

We developed a combination of technology for deposition contacts/wires upon RF sputtering InP films. In this way we demonstrate the possibility of fabrication the antennas and detectors. Indium phosphide (InP) films were deposited onto sapphire substrate using RF magnetron sputtering by varying the substrate temperature (50–100°C), under constant argon pressure (6.3•10^{-3} Bar) and RF power (100 W). The absorption coefficient versus photon energy for InP fims were measured at 300 K for three type of thickness, 500, 1000 and 2000 nm, respectively before and after HNO_3 etching. In figure 2 a, b, and c is presented the THz-TDS spectra for three different thicknesses, and insets represents the amplitude of THz pulse for etched vs initial samples.

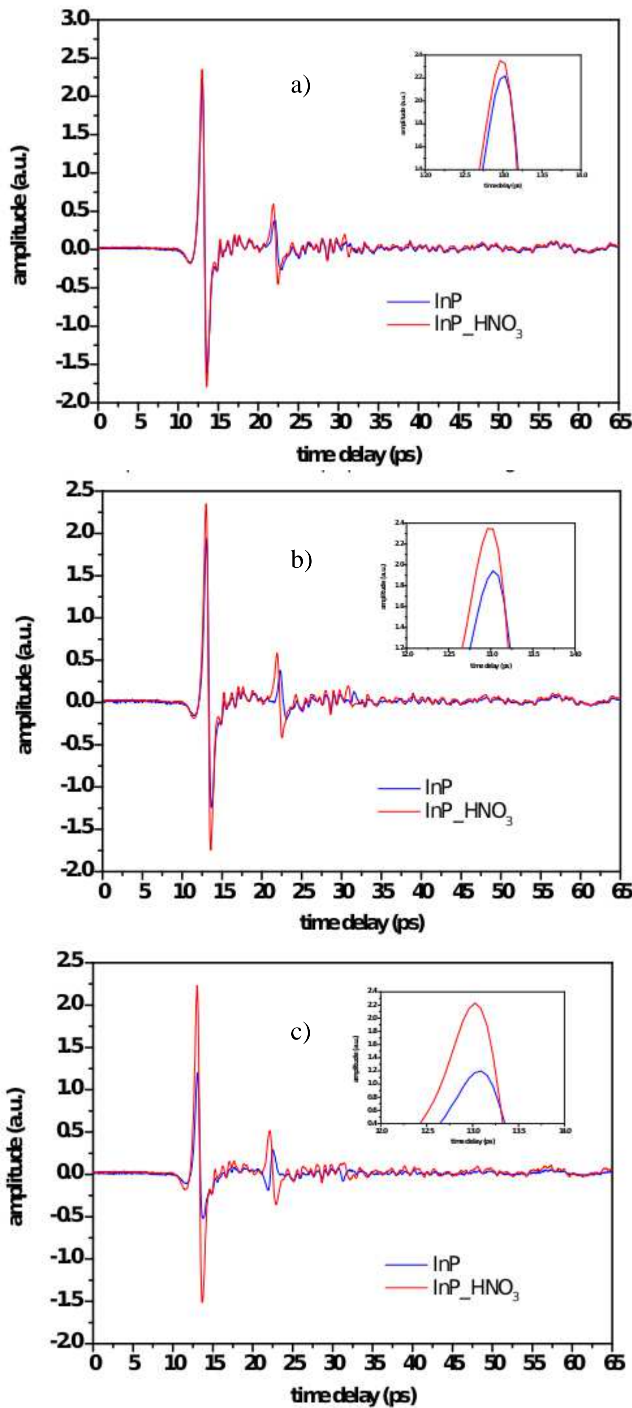

Fig. 2. THz TDS spectra for InP films in comparison with etched InP films with thickness of a) 500nm, b) 1000nm, and c) 2000nm respective.

According of early report of Aspnes and Studna [1983] the thickness of InP films were optimized for the absorption coefficient α [2]. As we can see from figure 3, the the slope of the absorption coefficient vs wavelength is changed after etching of indium layer wich remained after RF deposition. The power of IR lamp was ~180 (177) mW and optical pulses from a Femtolaser Fusion 20 pulsed laser at central wavelength of 805 nm have an average power of 180 mW. We report the surface impedance measurement of a magnetron RF sputtering InP films to be 15 MΩ/cm vs PCA 40-05-10-800-x from BATOP Optoelectronics one with 9 MΩ/cm, [3].

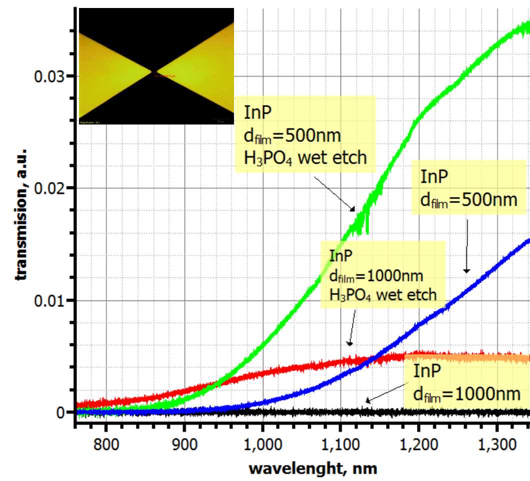

Fig. 3. IR spectra for InP films which correspond with thickness of 500 and 1000 nm before and after HNO_3 etching (inset is represented a butterfly antenna with gap inter-distance of 5 μm)

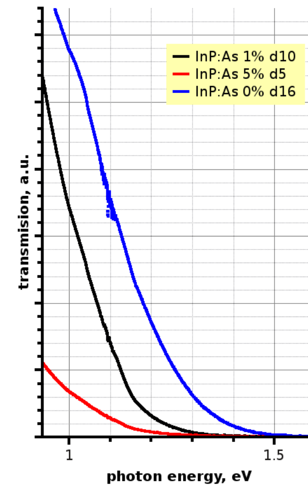

Fig. 4. IR spectra for InP films which correspond with doping level of As 0%, 1% and 5%

The InP film band gap is ~1.34 [4], 1.19 and 1.18 eV for As doping level of 0%, 1% and 5% respectively.

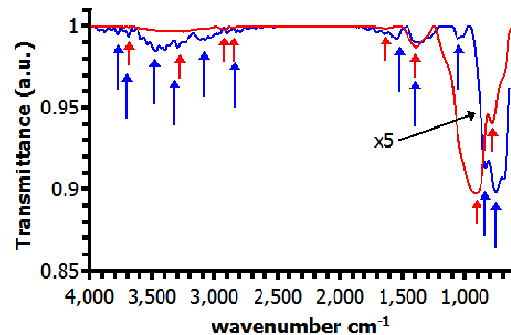

Fig. 5. FTIR spectra of InP thin film. The normalized spectrum of the InP annealed in Ar atmosphere for 30min at 450 °C is multiplied by factor 5 .

In the IR spectrum (figure 5) of the InP thin film, there is a stretching vibration peak of C-H hydroxyl group (the functional group in alcohols (ethanol, methanol, etc.)) at 2906cm^{-1}, in addition, there are peaks for In-H at 1356cm^{-1}, 1546 and 757cm^{-1}, P-H at 836 cm^{-1}. There are few changes after annealing in Ar atmosphere for 30min at 450 ^{o}C (see figure 5, the normalized spectrum): C-H at 2882cm^{-1}, In-H at 1397cm^{-1}, 1542 and 686cm^{-1}, P-H 855 and 686 cm^{-1}. We detect the peaks 1059 and 1025 cm^{-1}, respectively, related to the $InPO_4$ oxide formation after chemical and electro-chemical processes [5].

The Raman spectra were recorded by a Renishaw spectrometer using a 785 nm diode laser as excitation source. The Raman spectrum of InP thin film is presented in figure 6. The two relatively sharp peaks around 307 cm^{-1} and 343 cm^{-1} were assigned to the first-order scattering from TO and LO phonons of InP crystal, respectively, while weaker peaks at around 651 and 688 cm^{-1} were assigned to the second-order Raman scattering [6]. The observed strong and narrow LO phonon peak of InP is similar to that of the bulk and manifest a good crystalline quality of obtained films. The inset of figure 6 is presented the Raman LO peak intensity at different density of implanted of Ga ions, without implantation, 7•e^{22}, 1.4•e^{23} and 2.1•e^{23} cm^{-2}, respectively.

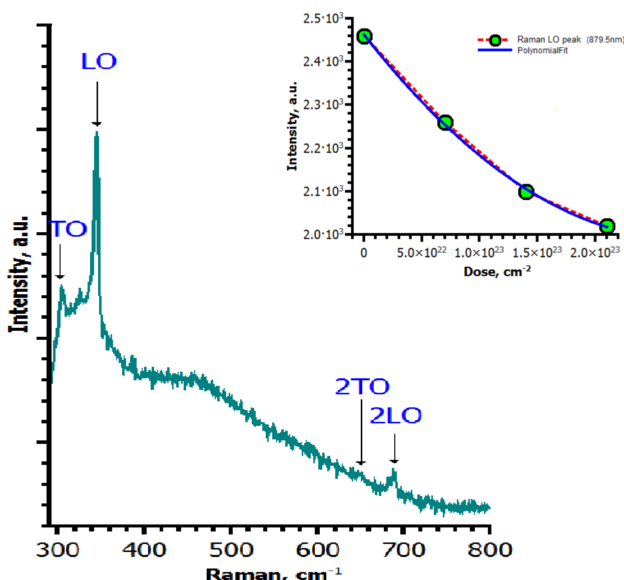

Fig. 6. Raman spectrum, inset is presented the Raman intensity vs density of implanted of Ga ions (Bristol, UK)

The Raman spectrum of the InP film, and we found a good correlation with literature [6]

The elemental composition of the films was determined by electron dispersive X-ray analysis using EDX, which consist of ~40%atoms of P and ~60%atoms of In. In order to increase the stoichiometry ratio (~50%atoms of P and ~50%atoms of In) we use two methods:

1. Changing the growing parameters for the RF sputtering deposition, and
2. Selective etching of In [7].

This result is seen in X-ray diffraction (figure 7 a,b,c,d). The thin film InP samples were deposited at 40W of RF power and 50, 65, 80 ^{o}C the growth temperatures were used. We can see that by decreasing the sample growth temperature the intensity of the In peak is decreasing (figure 9, a,b,c) The thin film obtained through this method remained amorphous (small crystallites ~1.8nm). A much better result was observed in the case of the selectively etched samples (figure 9, d), where X-ray diffraction spectra show well resolved InP peaks.

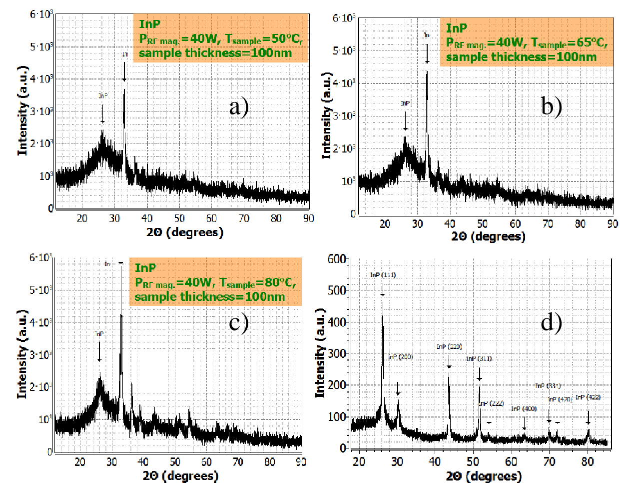

Fig. 7. XRD pattern for InP thin films.

The XRD measurement was performed with an X-ray diffractometer SmartLab Rigaku (IMT-Bucharest, RO) employing Cu Ka radiation from a rotating anode source and a Ge monochromator. As we can see from the Figure 7 a,b,c, the peaks for InP look broader than normally found for bulk material which is typical for small crystallites (the size is estimated by Williamson-Hall method, and it consist ~1.8 nm for samples from figure 7, a,b,c and ~20 nm for samples from figure 7 d). The indium peak is decreasing with temperature of film deposition.

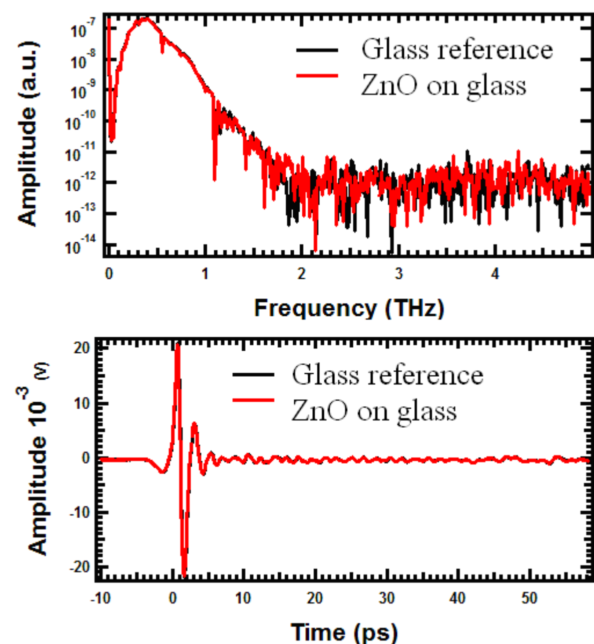

Fig. 8. THz spectra from glass and ZnO deposited on glass

The deposited ZnO film has a 400 nm thickness. In order to estimate the quality of deposited ZnO we studied the Raman scattering [8] and AFM. The roughness has been studied and it was found to be around 220 nm. That means that we have a variation of 400±220nm.

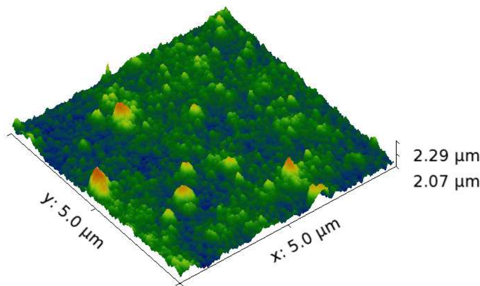

Fig. 9. 3D AFM image of ZnO deposited layer

Since ZnO films are promising for fabrication of THz devices, we tried to implement them into EWOD device. Recently THz birefringence has been reported [9].

The glass has been taken as reference material in studding the THz emission and it has been compared with the ZnO film deposited on the same glass (Fig. 8). One can see from the THz spectrum that significant changes do not occur. We suppose that the weak absorption is due to small thickness of the deposited film.

The final structure of EWOD chip is a transparent one for THz radiation and allows to scan easily any bio-fluid slipping through microchannel. The structure is obtained by thermal oxidation of a (100) Si wafer. The grown SiO_2 on top is 500 µm thick. A positive photoresist (PMMA) was used to configure Cr-Au pads, obtained by liftoff method. ZnO is deposited by RF magnetron sputtering.

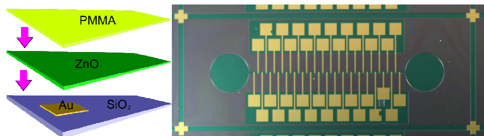

Fig. 10. Technological processes (left), and EWOD device photo (right)

In order to have a structure with hydrophobic surface we left the ZnO material on the surface of EWOD chip. As the undoped ZnO is considered dielectric one, $R=10^5$ Ω□, we remove it from external pads for contacting with microcontroller circuit.

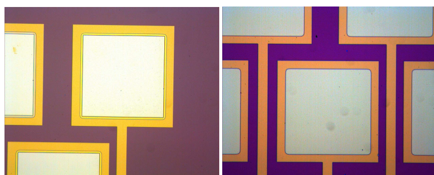

Fig. 11. ZnO removing from pads (left) before removing PMMA, and after (left)

6. CONCLUSION

We demonstrate the possibility to fabricate a device that is able to handle with liquids, and to measure the THz spectra in real time. We managed to dope the InP fims with As, 1% and 5% and we implanted different dose of Ga ions. The selective etching improve considerably the quality of InP films.

ACKNOWLEDGMENTS

This work was supported by Romanian – Moldavian 13.820.15.17/RoA (689) bilateral project, young scientist project 12.819.15.20A and partially supported by the FP7 project MOLD-ERA (Grant no 266515). I would like to thank for helping and supporting: A. Sarua, L. Ghimpu, A. Ionescu, A. Voiculescu and I. Tiginyanu.

RFERENCES

7. Lilian Sirbu, Lidia Ghimpu, Raluca Müller, Irina Vodă, Ion Tiginyanu, Veaceslav Ursaki, Traian Dascalu Hydrophobic ZnO used in EWOD technology and SAW devices for better bio-fluid slip at microchannel walls controlled by DC pulses, CAS2012, Proceedings, Vol.I, 15-17 oct 2012, Sinaia, Romania, p. 231-234.
8. Aspnes, D. E. and A. A. Studna, *Phys. Rev.* **B27**, 2 (1983) 985-1009
9. Datasheet for BATOP photoconductive antenna Available: www.batop.com/products/terahertz/photoconductive-antenna/data-sheet/manual_PCA-40-05-10-800.pdf
10. Band structure and carrier concentration of InP Available: http://www.ioffe.ru/SVA/NSM/Semicond/InP/bandstr.html
11. Olivier Pluchery, Joseph Eng Jr., Robert L. Opila, Yves J. Chabal, Etching And Oxide Formation On Inp Surfaces, Tenth International Conference on Vobrations at Surfaces, Palais du Grand Large, Saint Malo (France), June 17-21 2001
12. G. Irmer, Raman spectra of InP, in: Properties of indium phosphide, EMIS Datareview Series No.6, INSPEC: London and New York (1991), p.207
13. A.R. Clawson, Guide to references on III-V semiconductor chemical etching, Materials Science and Engineering, 31 (2001) 1-438
14. Zalamai V.V, Ursaki V.V., Rusu E., Arabadji P., Tiginyanu I.M., Sirbu L.. Photoluminescence and resonant Raman scattering in highly conductive ZnO layers. Applied Physics Letters, Vol. 84, Nr. 25, 2004, p. 5168-5170.
15. Youngchan Kim, Jaewook Ahn, Bog G. Kim, and Dae-Su Yee, Terahertz Birefringence in Zinc Oxide, Japanese Journal of Applied Physics 50 (2011) 030203